BATS, J. W., COPPENS, P. & KOETZLE, T. F. (1977). *Acta Cryst.* B**33**, 37–45.
BERGLUND, B., LINDGREN, J. & TEGENFELDT, J. (1978). *J. Mol. Struct.* **43**, 179–185.
BOTTOMLEY, F. & WHITE, P. S. (1979). *Acta Cryst.* B**35**, 2193–2195.
DITTMAR, G. & SCHÄFER, H. (1978). *Z. Naturforsch. Teil B*, **33**, 678–681.
FALK, H., HUANG, C. & KNOP, O. (1974). *Can. J. Chem.* **52**, 2380–2388.
FALK, H. & KNOP, O. (1973). *Water, a Comprehensive Treatise*, edited by F. FRANKS, Vol. 2, pp. 55–113. New York: Plenum Press.
FERRARIS, G. & FRANCHINI-ANGELA, M. (1972). *Acta Cryst.* B**28**, 3572–3583.
*Gmelins Handbuch der anorganischen Chemie* (1928). *Natrium*, System Nr. 21, 8th ed., pp. 958–960. Berlin: Verlag Chemie.
HAMILTON, W. C. & IBERS, J. A. (1968). *Hydrogen Bonding in Solids*. New York: Benjamin.
*International Tables for X-ray Crystallography* (1974). Vol. IV. Birmingham: Kynoch Press.
JOHNSON, P. L., KOCH, T. R. & WILLIAMS, J. M. (1977). *Acta Cryst.* B**33**, 1976–1979.
KOESTER, L. (1977). *Springer Tracts in Modern Physics – Neutron Physics*. Berlin: Springer.
LISENSKY, G. C. & LEVY, H. A. (1978). *Acta Cryst.* B**34**, 1975–1977.
MEREITER, K., PREISINGER, A. & GUTH, H. (1979). *Acta Cryst.* B**35**, 19–25.
MIKENDA, W. & PREISINGER, A. (1980). *Spectrochim. Acta Part A*, **36**, 365–370.
MIKENDA, W., PREISINGER, A. & STEIDL, H. (1981). *J. Raman Spectrosc.* Submitted.
PREISINGER, A., MEREITER, K., BAUMGARTNER, O., HEGER, G., MIKENDA, W. & STEIDL, H. (1981). *Inorg. Chim. Acta*. In the press.
RÉMY, F. & BACHET, B. (1968). *Bull. Soc. Chim. Fr.* pp. 3568–3569.
SHELDRICK, G. M. (1976). *SHELX* 76. Program for crystal structure determination. Univ. of Cambridge, England.
STEWART, J. M., KRUGER, G. J., AMMON, H. L., DICKINSON, C. & HALL, S. R. (1972). The XRAY system – version of June 1972. Tech. Rep. TR-192. Computer Science Center, Univ. of Maryland, College Park, Maryland.
WHALLEY, E. (1976). *The Hydrogen Bond*, Vol. 3, edited by P. SCHUSTER, G. ZUNDEL & C. SANDORFY, ch. 29, pp. 1426–1470. Amsterdam: North Holland.

*Acta Cryst.* (1982). B**38**, 408–415

# The Electronic Factors Linking the Structures of Graphite, Arsenic and Selenium

BY JEREMY K. BURDETT* AND JUNG-HUI LIN

*Department of Chemistry, The University of Chicago, Chicago, Illinois* 60637, *USA*

(*Received* 15 *October* 1980; *accepted* 4 *August* 1981)

## Abstract

The electronic structures of the graphite, arsenic and selenium arrangements are correlated with those of 'isoelectronic' molecules. The structural changes along the series are viewed in terms of simple molecular-orbital arguments, specifically the response of a parent structure to the presence of extra electrons (C → As → Se). Because of the extra symmetry present in the solid, the electronic explanation of the occurrence of puckered arsenic sheets is somewhat different from that used to view the trigonal pyramidal structure of ammonia.

## Introduction

One of the successes of modern theoretical chemistry has been the methodical analysis of the molecular-orbital structures of molecules (Gimarc, 1979; Hoffmann, 1981) and the development of simple ideas and theories to view structural, chemical and frequently mechanistic questions from a global viewpoint (Hoffmann & Woodward, 1970; Mingos, 1977; Burdett, 1980*b*). Much of this research has used approximate molecular-orbital methods such as the extended Hückel method (Hoffmann, 1963; Hoffmann & Lipscomb, 1962*a*,*b*) and the various 'NDO' schemes (Dewar, 1969). By way of contrast there is a scarcity of similar electronic descriptions of structural aspects of solids. Until recently these were limited to valence-bond arguments for tetrahedrally based molecules and

* Fellow of the Alfred P. Sloan Foundation and Camille and Henry Dreyfus Teacher–Scholar.

0567-7408/82/020408-08$01.00 

molecular studies on fragments of silicate structures (O'Keeffe & Navrotsky, 1981). In some recent studies we have employed many of the analytical tricks used in understanding structural aspects of molecules to view the structures of extended solid-state arrays. These include the use of the fragment formalism to understand features of solids involving puckered sheets of atoms (Burdett, 1980*a*), the application of the Woodward–Hoffmann methodology to view polymerization processes (Burdett, 1980*a*) and the discovery of a structurally important '*gauche*' effect (Wolfe, 1972) controlling the stabilities of solids such as arsenic and black phosphorus which may be derived by breakup of the rocksalt structure (Burdett, Haaland & McLarnan, 1982). In this paper we discuss the generation of some simple structures making comparisons between their theoretical descriptions and those of isoelectronic molecules. Comparisons of this type are of course not new – qualitatively such ideas are of widespread use in crystal chemistry – but are viewed here in a fresh light.

## Methodology and philosophy

We use a method described in a previous paper (Burdett, 1980*a*) to generate the molecular orbitals of a fragment-within-the-solid. With reference to (1), which

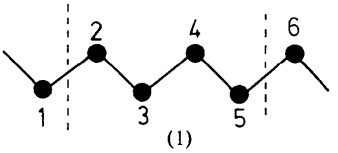


(1)

shows a simple one-dimensional chain, the molecular orbitals of a fragment containing one or two repeat units will not well represent the electronic environment in the solid since this collection of atoms has potent orbitals at each end, which, in the solid, are used for the attachment of the fragment to its surroundings. In order to overcome this problem we tie the ends of the fragment (atoms 2 and 5) together by imposing cyclic boundary conditions on the molecular-orbital calculations. Zunger has called the approach the small-periodic-cluster method (Zunger, 1974) and Messmer and co-workers have used it to study chemisorption on graphite-like sheets (Messmer, McCarroll & Singal, 1972). The resultant orbitals are actually the orbitals of a band-structure calculation at $\mathbf{k} = 0$ if one repeat unit of the structure is chosen. With larger fragments the orbitals at other points in $\mathbf{k}$ space begin to be included. The method, while perhaps of limited practical importance, does provide an important conceptual link between the results of the band-structure calculation and the orbital structure of simple molecules. Once these orbitals are obtained then the techniques of analysis developed in recent years for viewing the electronic structures of molecules may be exploited to view the solid state in an analogous way.

## Graphite

This simple system (Fig. 1) has attracted attention because of its simplicity. Planar $6^3$ sheets are found for graphite itself and also for the isoelectronic system BN. Similar sheets are found in the $AlB_2$ structure held together by aluminum atom 'spacers'. The most recent band-structure calculation is that of Whangbo, Hoffmann & Woodward (1979) using the extended Hückel method. We will use the same technique in this paper to underwrite the ideas we present. The parameters and other details of the calculations are given in the Appendix. Fig. 2(*a*) shows the results of such a calculation on this system. The conducting (semimetallic) properties of graphite are clearly indicated by the level crossing at the point $K$ in $\mathbf{k}$ space (2) or the touching of filled and empty bands with four

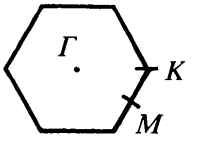


(2)

electrons per atom. A feel for the reasons influencing the construction of this diagram may be obtained by looking at the fragment-within-the-solid orbitals of increasingly complex fragments. The repeat unit of the structure is simply the pair of atoms $u$, $v$ (3). Each lies

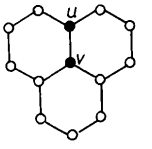


(3)

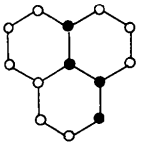

(4)

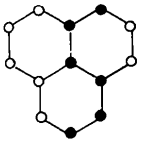

(5)

at a site of $D_{3h}$ symmetry. Tying the ends of this unit together in two dimensions leads to the very simple molecular-orbital diagram of Fig. 3 which represents the band structure at $\Gamma, \mathbf{k} = 0$. Each atom lies at a site of $D_{3h}$ symmetry and so the valence atomic orbitals transform as $a_1'(s)$ and $a_2'' + e'(p)$. There are then a pair (bonding and antibonding respectively) of $a_1'$ orbitals arising purely *via* $s$-orbital overlap on the two centers, two sets of in-plane degenerate $e'$ $\sigma$ orbitals

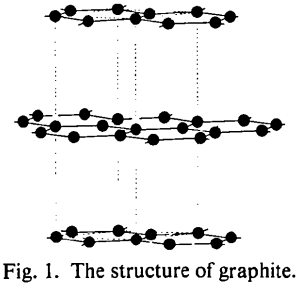

Fig. 1. The structure of graphite.

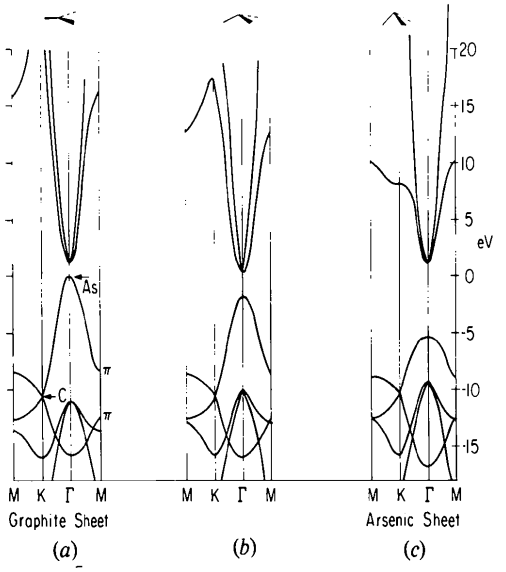


Fig. 2. The band structures of (*a*) graphite, (*c*) arsenic and (*b*) a geometry between the two.

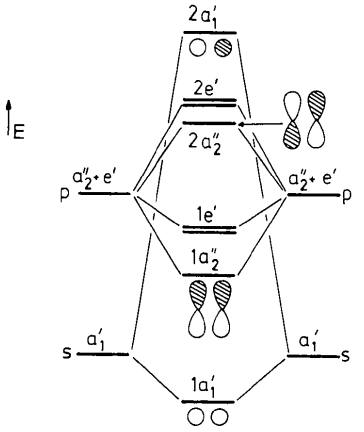


Fig. 3. The generation of the fragment-within-the-solid orbitals of a two-atom graphite unit (3).

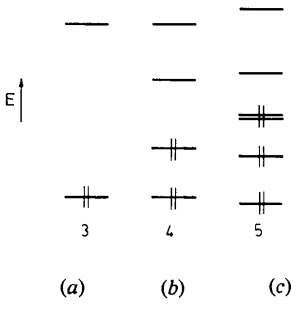


Fig. 4. The fragment-within-the-solid orbitals of the graphite fragments of (3), (4) and (5). Only the $\pi$-type orbitals are shown.

and a pair of out-of-plane $a_2''$ $\pi$ orbitals. Filling these orbitals with four electron pairs leads to the configuration $(1a_1')^2(1e')^4(1a_2'')^2$ where no antibonding orbitals are occupied. Choice of a larger unit, such as that of (4), gives rise to a larger number of orbitals (Fig. 4*b*) where, with the relevant number of electrons (eight pairs), none of the $\pi^*$ orbitals are occupied. For the six-atom fragment (5), however, a degenerate pair of $\pi$ orbitals is found which are only half filled (Fig. 4*c*). Here is the fragment-within-the-solid analog of the band-structure result noted above where the system is a conductor (semimetal) as a result of level crossing in **k** space. The use of an even larger fragment, for example the eighteen-atom raft of Messmer *et al.* (1972) and Messmer & Watkins (1973), is able to fill in the orbitals at many more points in **k** space. The technique is a useful way to stimulate a solid surface in calculations aimed at studying electronic effects involved in chemisorption.

It is interesting to ask how such a level crossing can be eliminated. Our argument is not a new one but can usefully be restated. Since the higher energy, at $\Gamma$, of the two $\pi$ bands is antibonding between the two atoms $u,v$ for the fragment (4), replacement of this $C_2$ unit by a pair of atoms of disparate electronegativity ($AX$) will increase the separation between the two $a_2''$ levels of Fig. 3 and push the higher-energy $\pi$ levels of Fig. 4 to higher energy. This simply occurs because the primarily bonding levels will be largely $X$ located (and hence at low energy) and the primarily antibonding levels will be largely $A$ located (and hence the high energy). Such a situation is found in BN, which, isoelectronic with graphite, is an insulator. Here the two bands do not cross.

## Arsenic

Arsenic with five electrons per atom, contains puckered graphite-like sheets (Fig. 5). Similar units are found in the structure of $CaSi_2$ where the sheets are linked by calcium (ion) spacers. Many structures, including those of sphalerite, wurtzite and GaS, may be built up by linking such sheets together (Burdett, 1980*a*). With one more electron per atom than graphite, the $2a_2''$ $\pi^*$ orbital of Fig. 3 and the higher-energy $\pi$ band of Fig.

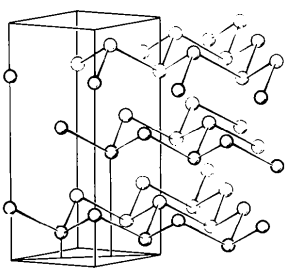

Fig. 5. The structure of arsenic.

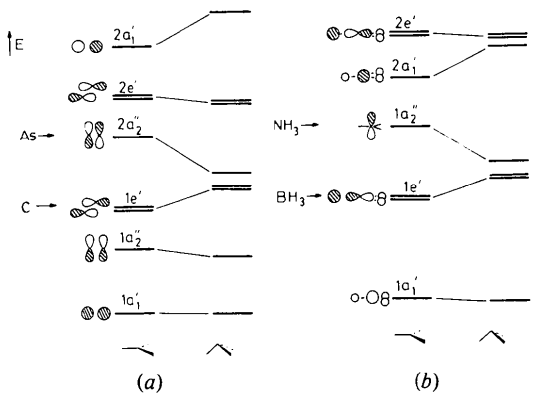


Fig. 6. Walsh diagrams showing the energy changes of (*a*) the fragment-within-the-solid orbitals of graphite on puckering the structure and (*b*) the molecular orbitals of $AH_3$ molecules. The HOMO corresponding to graphite, arsenic, $BH_3$ and $NH_3$ are shown.

$2(a)$ are completely filled. At the point $\Gamma$ this level is close in energy to the degenerate ($e'$) $\sigma$ antibonding orbital. Much higher in energy lies the $\sigma$ antibonding $a_1'$ orbital. Extended Hückel calculations are notorious for placing such levels very high in energy and this level ordering should accordingly be viewed with caution. The band-structure calculation for the graphite structure by Painter & Ellis (1970), for example, shows a situation where the three antibonding orbitals of Fig. 3 ($2a_2''$, $2e'$ and $2a_1'$) are quite close in energy.

The changes in the orbital energies of Fig. 3 on distortion are shown in a Walsh diagram in Fig. 6. Also shown are the analogous energy changes for pyramidalization of an $AH_3$ molecule. There are clearly great similarities between the two. Fig. 2 shows how the band-structure energies change on distortion. Before proceeding further to uncover the electronic reasons behind these energy changes on pyramidalization for the solid system we discuss those for the simpler molecular case.

$BH_3$ with six valence electrons is a planar molecule, but $NH_3$ with eight electrons is pyramidal. Energetically, the distortion away from planar is therefore determined by the behavior of the $2a_2''$ orbital of Fig. 6(*b*) which is the HOMO (highest occupied molecular orbital) for $NH_3$. Such energy changes are usefully viewed in terms of perturbation theoretical arguments. The perturbation in our case is the distortion away from the planar geometry. First-order changes are associated with the changes in overlap integrals between the orbitals of the central atom and ligands. Second-order energy changes are associated with the mixing together of orbitals, which may be of different symmetry in the parent structure but which transform as the same symmetry species on distortion. Perturbation theory tells us that such energetic effects will be inversely proportional to the energy difference between the two mixing orbitals before the perturbation is switched on.

Equation (1) gives an expression for the energy change associated with an orbital $i$, on mixing with an orbital $j$, as the result of the distortion perturbation $(\partial\mathscr{H}/\partial q)_0 q$, where $q$ is the distortion coordinate.

$$\Delta E_i = \frac{[\int \psi_i (\partial\mathscr{H}/\partial q)_0 \psi_j \mathrm{d}\tau]^2}{E_i - E_j} q^2. \qquad (1)$$

If $|E_i| > |E_j|$ (*i.e.* orbital $i$ lies deeper in energy than orbital $j$), then the result will be stabilization of orbital $i$. Similarly, if $|E_i| < |E_j|$, the reverse is true and orbital $i$ is destabilized. The general result is that the two orbitals 'repel' each other in energy as the perturbation is switched on. Specifically, in the case of $NH_3$ we are interested in the mixing together of $1a_2''$ and $2a_1'$ orbitals of the planar structure on distortion and identify orbital $i$ with the HOMO and orbital $j$ with the LUMO (lowest unoccupied molecular orbital). Parenthetically we note that there is a symmetry restriction on the nature of the distortion coordinate $q$ for a nonzero numerator in equation (1). In this case $q$ is the out-of-plane bending mode of planar $NH_3$ of species $a_2''$ which is just of the right symmetry to couple $2a_1'$ and $1a_2''$ orbitals. In general, equation (1) should contain a summation over all higher-energy orbitals $j$ instead of a single term involving the LUMO. Some possibilities will be excluded by this symmetry restriction and very-high-energy orbitals may be neglected because of the large energy gap appearing in the denominator. Such symmetry-based approaches to the geometries of the main-group $AY_n$ molecules have been discussed by Bartell (1968) and Pearson (1969, 1970*a*,*b*) under the umbrella of the second-order Jahn–Teller effect.

Equation (1) suggests, then, that the driving force for distortion away from the planar $AH_3$ geometry will be inversely proportional to the HOMO–LUMO gap of the planar structure. The relative magnitudes of the inversion barriers in $NH_3$ (small) and $PH_3$ (larger) have been rationalized on this basis aided by the results of *ab initio* calculations (Levin, 1975). In $PH_3$ the energy gap is smaller at the planar structure than for $NH_3$. In addition the influence of $\pi$ orbitals and ligand electronegativity on the bond angle may be approached in a similar fashion (Bartell, 1968). Increasing the ligand orbital ionization potentials (increasing electronegativity difference, $\Delta\chi$ in the Mulliken sense) leads to a shifting to lower energy of the entire $\sigma$ manifold of orbitals (6) with a corresponding drop in the size of

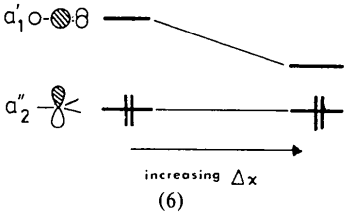


(6)

$E_{HOMO} - E_{LUMO}$. As a result, the general trend is to smaller $XNX$ angles in $NX_3$ systems as the electronegativity of $X$ increases. The planarity of $CH_3$ but increasing pyramidality of $CH_xF_{3-x}$ ($x = 0, 1, 2$) as $x$ decreases may be due to a similar effect. The inclusion of filled, deep-lying $\pi$ orbitals on the ligands leads to the nonbonding HOMO in $AH_3$ becoming $\pi$ antibonding between central atom and ligands with a corresponding decrease in the HOMO–LUMO gap (7)

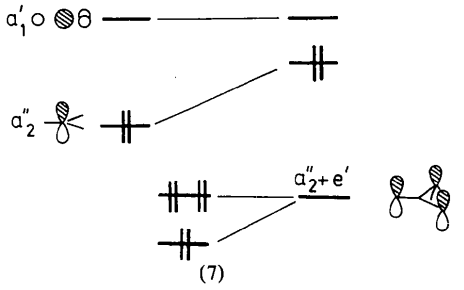


(7)

which aids the bending process in a similar fashion. Adding empty higher-energy $\pi$ orbitals to the diagram results in an increased gap (8) and a decreased tendency to bend.

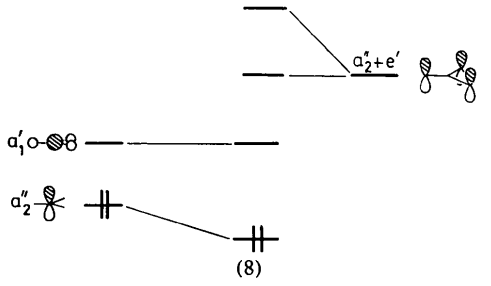


(8)

Such may well be the case in $N(SiH_3)_3$ which is planar. In $O(SiH_3)_2$ and isoelectronic phosphonium ylides, analogous ideas, supported by *ab initio* results, allow a rationalization of bond angles lying between tetrahedral [expected on VSEPR grounds (Gillespie, 1972)] and linear (Albright, Hoffman & Rossi, 1980). In silicate structures a wide range of Si–O–Si angles are found. In coesite one of the angles is 180° (Gibbs, Prewitt & Baldwin, 1977).

In such $AX_3$ systems, where $X$ is a $\pi$-bearing ligand, there are also first-order changes in the energy on bending which may stabilize or destabilize the planar geometry. For $\pi$ donor ligands $X$ (7) where the HOMO is $\pi$ antibonding (9) between $A$ and $X$ such destabilization is relieved on bending (*e.g.* in $NF_3$). In the case of $N(SiH_3)_3$ the reverse is true. The $\pi$ stabilization of the planar structure (10) decreases on

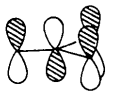

(9)

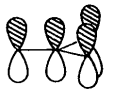

(10)

pyramidalization. In the molecular case both first-order and second-order effects involving these $\pi$ orbitals work together to either stabilize ($\pi$-acceptor ligands) or destabilize ($\pi$-donor ligands) the planar geometry.

We are now in a position to view the structural change from graphite to arsenic. The behavior of the degenerate $e'$-type orbitals of Fig. 6 on pyramidalization is similar in the two cases. The lower-energy bonding pair $1e'$ is expected to be destabilized on bending as the overlap between the central atom and ligand orbitals decreases. (This is most easily seen in the molecular example shown in Fig. 6*b*.) The opposite should be true for the higher-energy antibonding $2e'$ pair. On bending, these orbitals will become less antibonding. There is another energetic effect, a destabilization of both sets of $e'$ orbitals on distortion as the ligand orbitals themselves overlap in an out-of-phase manner. The overall result is a small energy change for the higher-energy $e'$ pair, and a large energy destabilization for the bonding pair where these two destabilizing effects reinforce each other. The behavior of the $a_2''$ and $a_1'$ graphite orbitals is more interesting and shows some important differences when compared to the molecular case. On distortion their symmetry is lowered to $a_1$ such that *sp* mixing may occur between them. In the molecular case we have just described, this is dominated by that occurring between $1a_2''$ and $2a_1'$. In these solid-state structures there is, however, an extra element of symmetry not possessed by the molecular analog – a centre of symmetry, located at the midpoint of each C–C (Fig. 1) or As–As linkage (Fig. 5). Thus, each level, in addition to its point-symmetry label, also carries a $g$ or $u$ label which describes its properties with respect to such inversion. (This is true at all points in **k** space too.) Following the symmetry restriction of equation (1) noted above, the lower-energy arsenic $a_1$ ($g$ or $u$) orbital in each case is stabilized by *sp* mixing and the higher-energy orbital of the same symmetry is destabilized (11). In addition

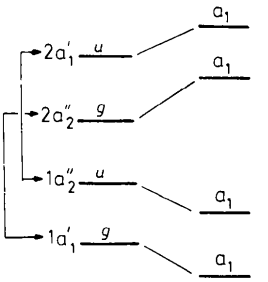


(11)

there are first-order energy changes on distortion associated with the $\pi$-type orbitals of $a_2''$ symmetry which are simply determined, as in the molecular case of $NF_3$ and $N(SiH_3)_3$, by the phase relationship between $\pi$ orbitals on adjacent centers. A summary of the molecular-orbital effects influencing the behavior

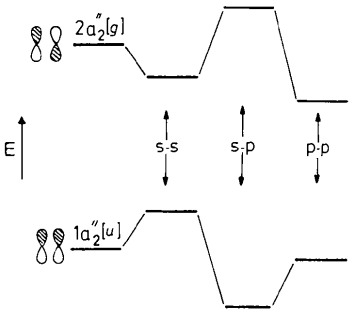


Fig. 7. Summary of the energetic effects controlling the $a_2''$ orbitals on bending from an analysis of the composition of these orbitals in the arsenic structure. The first two contributions (*via* $s$–$s$ and $s$–$p$ overlap) arise *via* admixture of $s$ orbitals into these orbitals, purely $p$ at the graphite structure on bending. The third contribution is the first-order energy correction from $p$–$p$ overlap changes on distortion.

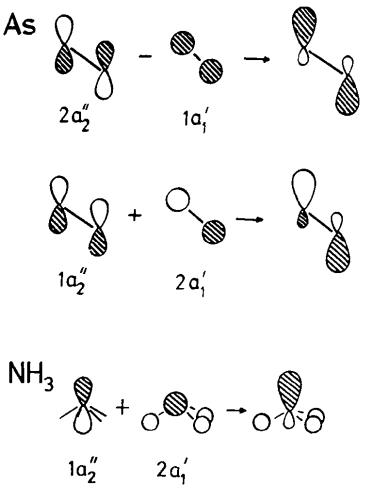


Fig. 8. $sp$ mixing according to the rules of perturbation theory, which generates lone pairs on puckering the graphite sheet.

of these $a_2''$ orbitals is shown in Fig. 7. We have divided the energy changes into three parts, that due to $s$–$s$ and $s$–$p$ overlap on adjacent centers which are the two energetic results of $sp$ mixing, and the first-order changes associated with the change in $p$–$p$ $\pi$-type overlap. For the $1a_2''$ ($u$) orbital which is stabilized overall by $sp$ mixing note that the $s$–$s$ contribution is destabilizing owing to admixture of the antibonding $2a_1'$ ($u$) orbital. Similarly, the $2a_2''$ ($g$) orbital, destabilized overall by $sp$ mixing, receives a stabilizing contribution *via* $s$–$s$ overlap since it mixes with the bonding $1a_1'$ ($g$) orbital. We can see from this diagram (Fig. 7) the reason for the quantitative result of Fig. 2 that the $1a_2''$ orbital is stabilized less on bending than the higher-energy $2a_2''$ orbital.

The directions of the energetic changes calculated in Fig. 6*a* and their dissections in Fig. 7 show that it is the first-order contribution to the energy *via* changes in the $p\pi$–$p\pi$ overlap integral which determines the puckered geometry of solid arsenic compared to that of graphite. The pyramidal structure around each arsenic atom is then due to the dominance of changes in $\pi$ bonding rather than $sp$ mixing in the sense of a second-order Jahn–Teller distortion used above to view the structure of $NH_3$ and $PH_3$. This is a result which is perhaps unexpected. $sp$ mixing does of course occur on pyramidalization as the local symmetry is lowered (energetically it clearly contributes to Fig. 7) and we may use perturbation-theory arguments to see how the nature of the orbitals changes as a result. Since the lower energy of two interacting orbitals is stabilized as they mix together, this implies that the higher-energy orbital mixes into the lower in a bonding way. In a similar fashion, the lower-energy orbital mixes into the higher-energy one in an antibonding way, leading to a destabilization of the latter (Hoffmann, 1971). With these very simple ideas Fig. 8 shows how $s,p$ mixing occurs to produce a pair of lone-pair orbitals $2a_1$, $3a_1$ and a strongly antibonding $4a_1$ orbital. The composition of the lowest $a_1$ orbital changes only slightly on pyramidalization. A very similar picture showing generation of lone-pair orbitals is found at the special point of the Brillouin zone (Baldereschi, 1973). The analogous production of the ammonia lone pair on bending is also shown.

To conclude this section we may say that the planar graphite structure is stable at its geometry for the case of four electrons per atom since both $\sigma$ bonding (*via* the $e'$ symmetry orbitals of Fig. 3) and $\pi$ bonding is best here. This is in spite of the fact that $sp$ mixing works to stabilize the pyramidal geometry *via* the stabilization of the $1a_2''$ orbital on bending. With five electrons per atom, on the other hand, the pyramidal arsenic structure is more stable since $\pi$-antibonding [$2a_2''$ ($g$)] effects in the HOMO are relieved. This is in spite of the fact that the $sp$ mixing works to destabilize the HOMO on bending.

## Selenium

Selenium contains one more electron per atom than arsenic and its structure (Fig. 9) may be considered to be derived from that of the arsenic layer arrangement by selectively breaking one linkage around each arsenic atom such that chains of atoms are produced (Burdett, 1979) [or, alternatively (Harrison, 1980), *via* the breakup of the rocksalt structure]. Followed by a small rotation about one of the linkages the observed spiral structure of elemental selenium and tellurium and of fibrous sulfur is produced. We may again view the structure in electronic terms as the result of occupation of high-energy orbitals of the arsenic structure when each atom contributes six valence electrons to the

structure. Fig. 10 shows the effect of the bond-breaking distortion on the band structure of the solid. The diagram for the arsenic structure is different from that of Fig. 2. Here we have only shown the electronic structure for values of **k** lying in the same direction as that eventually describing the chain or spiral structures after bond fission. The highest-energy orbitals occupied for the arsenic structure with the selenium configuration are antibonding between adjacent atoms. As the structure is split apart their character changes to lone-pair orbitals located at lower energy. This dramatic stabilization is the dominant feature of the diagrams of Fig. 10. Clearly, the band-structure energy from this figure is lower for the spiral (observed) geometry than for the simple chain structure obtained by bond fission of the arsenic layer structure. The factors determining this geometrical choice are actually quite straightforward. The fragment-within-the-solid orbitals of the one-dimensional systems are very similar to the molecular orbitals of $A_2X_2$ molecules (Gimarc, 1979). Just as $(CH)_n$, isoelectronic with the hypothetical species $N_n$, is a planar but nonlinear system, so $N_2F_2$ is a planar molecule with *cis* and *trans* isomers. Similarly, with two more electrons, just as $S_2F_2$, $O_2F_2$ and $O_2H_2$ have a skewed nonplanar geometry, so the selenium prefers the spiral arrangement where the dihedral angle associated with a contiguous group of four atoms is close to 90°. Such a '*gauche* effect' is of course observed in other molecules such as $N_2H_4$ and $P_2H_4$ (Wolfe, 1972). It is perhaps an unlikely atomic configuration at first sight, since the *gauche* arrangement of lone pairs is, on VSEPR grounds (Gillespie, 1972), expected to be of higher energy than the *trans* arrangement. There is, however, a relatively simple orbital explanation for the stability order *gauche* > *trans* > *cis*. We refer the reader to a study by Wolfe (1972) for a discussion of the problem. We have shown how a similar *gauche* effect is structurally very important in determining structures (including that of arsenic) derived from rocksalt by selective fission of three mutually perpendicular linkages.

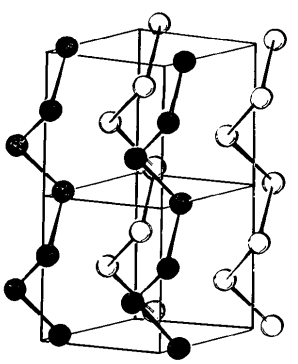

Fig. 9. The chain structure of selenium.

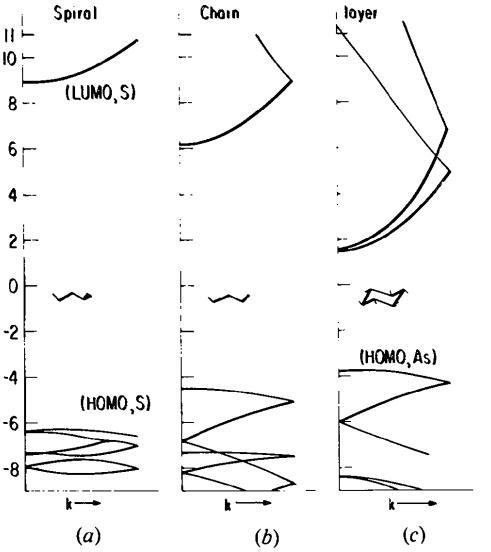


Fig. 10. (*a*) The band structure of arsenic, (*b*) the effect of breaking one linkage around each center, and (*c*) the band structure of the observed spiral arrangement.

We thank the donors of the Petroleum Fund, administered by the American Chemical Society, for their partial support of this research.

## APPENDIX

All calculations were of the extended Hückel type (Hoffmann & Lipscomb, 1962*a*,*b*; Hoffmann, 1963). The band-structure program was written by M.-H. Whangbo whom we thank for permission to use it. An interatomic separation of 1·575 Å was used in every case and the band structures of Figs. 2 and 10 used atomic-orbital input parameters, $H_{ii}$ values and exponents in parentheses relevant for carbon: 2*s*, −21·4 eV (1·625); 2*p*, −11·4 eV (1·625). The qualitative features of these diagrams were similar if phosphorus or arsenic parameters were used instead. All calculations for arsenic and graphite were performed on single isolated sheets.

### References

ALBRIGHT, T. A., HOFFMAN, P. & ROSSI, A. R. (1980). *Naturforscher*, B**35**, 34–40.

BALDERESCHI, A. (1973). *Phys. Rev. B*, **7**, 5212–5215.

BARTELL, L. S. (1968). *J. Chem. Educ.* **45**, 754–767.

BURDETT, J. K. (1979). *Nature (London)*, **279**, 121–125.

BURDETT, J. K. (1980*a*). *J. Am. Chem. Soc.* **102**, 5458–5462.

BURDETT, J. K. (1980*b*). *Molecular Shapes*. New York: John Wiley.

BURDETT, J. K., HAALAND, A. & MCLARNAN, A. (1982). *J. Chem. Phys.* In the press.

DEWAR, M. J. S. (1969). *The Molecular Orbital Theory of Organic Chemistry*. New York: McGraw-Hill.
GIBBS, G. V., PREWITT, C. T. & BALDWIN, K. J. (1977). *Z. Kristallogr.* **145**, 108–115.
GILLESPIE, R. J. (1972). *Molecular Geometry*. London: Van Nostrand–Rheinhold.
GIMARC, B. M. (1979). *Molecular Structure and Bonding*. New York: Academic Press.
HARRISON, W. (1980). *Electronic Structures of Solids*. San Francisco: Freeman.
HOFFMANN, R. (1963). *J. Chem. Phys.* **39**, 1397–1412.
HOFFMANN, R. (1971). *Acc. Chem. Res.* **4**, 1–9.
HOFFMANN, R. (1981). *Science*, **211**, 995–1007.
HOFFMANN, R. & LIPSCOMB, W. N. (1962*a*). *J. Chem. Phys.* **36**, 2179–2189, 3489–3493.
HOFFMANN, R. & LIPSCOMB, W. N. (1962*b*). *J. Chem. Phys.* **37**, 2872–2883.
HOFFMANN, R. & WOODWARD, R. B. (1970). *The Conservation of Orbital Symmetry*. Weinheim: Verlag Chemie.
LEVIN, C. C. (1975). *J. Am. Chem. Soc.* **97**, 5649–5655.
MESSMER, R. P., MCCARROLL, B. & SINGAL, C. M. (1972). *J. Vac. Sci. Technol.* **9**, 891–897.
MESSMER, R. P. & WATKINS, G. D. (1973). In *Radiation Damage and Defects in Semiconductors, Conf. Ser.* No. 16. London: Institute of Physics.
MINGOS, D. M. P. (1977). *Adv. Organomet. Chem.* **15**, 1–51.
O'KEEFFE, M. & NAVROTSKY, A. (1981). *The Structure of Complex Solids*. New York: Academic Press.
PAINTER, G. S. & ELLIS, D. E. (1970). *Phys. Rev. B*, **1**, 4747–4752.
PEARSON, R. G. (1969). *J. Am. Chem. Soc.* **91**, 1252–1254, 4947–4955.
PEARSON, R. G. (1970*a*). *J. Chem. Phys.* **52**, 2167–2174.
PEARSON, R. G. (1970*b*). *J. Chem. Phys.* **53**, 2986–2987.
WHANGBO, M.-H., HOFFMANN, R. & WOODWARD, R. B. (1979). *Proc. R. Soc. London Ser. A*, **366**, 23–46.
WOLFE, S. (1972). *Acc. Chem. Res.* **5**, 102–111.
ZUNGER, A. (1974). *J. Phys. C*, **7**, 76, 96–106.